KAUNAS UNIVERSITY OF TECHNOLOGY
VYTAUTAS MAGNUS UNIVERSITY

GINTARĖ VAIDELIENĖ

WAVELET-BASED APPROACH TO THE DETECTION OF DEFECTS IN TEXTURE IMAGES: THEORETICAL AND PRACTICAL ASPECTS

Summary of doctoral dissertation
Physical Sciences, Informatics (09P)

2017, Kaunas

KAUNO TECHNOLOGIJOS UNIVERSITETAS
VYTAUTO DIDŽIOJO UNIVERSITETAS

GINTARĖ VAIDELIENĖ

TEKSTŪRINIŲ VAIZDŲ KOKYBĖS ĮVERTINIMAS SPEKTRINĖJE DISKREČIŲJŲ BANGELIŲ SRITYJE: TEORINIAI IR PRAKTINIAI ASPEKTAI

Daktaro disertacijos santrauka
Fiziniai mokslai, informatika (09P)

2017, Kaunas

Disertacija rengta 2012–2017 metais Kauno technologijos universitete Matematikos ir gamtos mokslų fakultete, Taikomosios matematikos katedroje.

Mokslinis vadovas:

Prof. dr. Jonas VALANTINAS (Kauno technologijos universitetas, fiziniai mokslai, informatika, 09P).

Redagavo: Dovilė Dumbrauskaitė (leidykla „Technologija")

Informatikos mokslo krypties disertacijos gynimo taryba:

Prof. habil. dr. Rimantas BARAUSKAS (Kauno technologijos universitetas, fiziniai mokslai, informatika, 09P) – **pirmininkas**;
Prof. habil. dr. Juozas AUGUTIS (Vytauto Didžiojo universitetas, fiziniai mokslai, informatika, 09P);
Prof. habil. dr. Genadijus KULVIETIS (Vilniaus Gedimino technikos universitetas, fiziniai mokslai, informatika, 09P);
Prof. habil. dr. Minvydas Kazys RAGULSKIS (Kauno technologijos universitetas, fiziniai mokslai, informatika, 09P);
Prof. dr. Miguel A. F. SANJUAN (Rey Juan Carlos universitetas, Ispanija, fiziniai mokslai, informatika, 09P).

Disertacija bus ginama viešame infomatikos mokslo krypties disertacijos gynimo tarybos posėdyje 2017 m. gegužės 19 d. 10 val. Kauno technologijos universiteto Rektorato salėje.

Adresas: K. Donelaičio g. 73-(402), 44249 Kaunas, Lietuva.
Tel. (370) 37 300 042; faks. (370) 37 324 144; el. paštas doktorantura@ktu.lt.

Disertacijos santrauka išsiųsta 2017 m. balandžio 19 d.
Disertaciją galima peržiūrėti internete (http://ktu.edu), Vytauto Didžiojo universiteto (K. Donelaičio g. 52, Kaunas) ir Kauno technologijos universiteto (K. Donelaičio g. 20, Kaunas) bibliotekose.

ACKNOWLEDGEMENTS

I am grateful to the staff of the Department of Applied Mathematics for the opportunity to aspire to the PhD studies.

I would like to express my special appreciation and thanks to my advisor Professor Dr. Jonas Valantinas for the opportunity to work together, for encouraging my research and for allowing me to grow as a research scientist. Your advice on research have been priceless and your guidance has helped me during the time of research and writing of this thesis.

My deepest feelings and gratitude are sent to my husband, family and friends. Thank you for your patience, support and love.

I also place on record, my sense of gratitude to one and all who, directly or indirectly, have helped me during research and writing of this thesis.

INTRODUCTION

Over the last decades, the interest in the digital image analysis has increased considerably. Images as the most perceivable form of information have gained strong involvement in such fields as medicine, microscopy, astronomy, robotics, defence industry, etc.

Interpretation, analysis and processing of the human perception of images and realization of the analogous action mechanism on computers are rapidly increasing. Improvements in computer technology have made it possible to implement and practically apply complex image processing techniques and methods. It is essential to replace human activities in spheres requiring a long and tense human labour under difficult conditions. Quality control optimization of the industrial process which often relies on visual analysis of digital images is one of such fields.

Quality control carries great importance in today's competitive industry. International standard ISO 9000 describes quality as a "set of production properties and characteristics of services which allows satisfying the stated or implied requirements".

One of the approaches to improve the quality of the final product is ensuring effectiveness at each stage of the production process. Usually, it is humans (inspectors) who are responsible for detecting defects on the surfaces of various industrial products. However, this method is very subjective and it slows down the production process, thus it is both costly and time consuming. It is estimated that human productivity in determining the quality of the product is 60–75 %. Therefore, it is important to develop and computerise efficient defect detection techniques for texture images.

The texture defect detection techniques (in images of paper, glass sheets, ceramic tiles, fabrics, leather, plastic products and other) are closely related to the digital image processing procedures. Literature sources present many various approaches and technologies to tackle this issue. All of them can be divided into the following groups: statistical, spectral texture analysis, model-based and structural approach. Also, methods for detecting specific defects, such as holes, stains, fractures or colour tones can be distinguished. Currently, a need for systems which could analyse and identify various textures and a wide range of their defects is growing.

This dissertation proposes a novel defect detection technique for texture (surface) images. The developed technique is implemented in the spectral discrete wavelet domain. It is worth emphasizing that nowadays discrete wavelets represent the most popular and effective method of analysis. The proposed technique for detecting texture defects is successfully applied for the analysis of actual texture surfaces and their quality control.

The object of the research: texture surface (image) classification techniques based on the discrete wavelet theory.

The aim of the research: to develop a new flexible (parameterized) system for assessing the quality of texture images in the spectral discrete wavelet domain and adjust the system to actual quality testing environments.

Objectives of the research

In order to achieve the aim of the research, the following objectives were set:

(1) To develop criteria for detecting texture defects in the spectral discrete wavelet domain and provide the methodology;

(2) To investigate the possibilities of applying various discrete wavelet transforms (DWT) for determining the quality of texture images;

(3) To develop an algorithm for fast calculation of DWT spectra for given fragments of texture images;

(4) To propose an effective technique for texture defect localization;

(5) To develop a parameterized system for testing texture images and localizing the detected defects;

(6) To investigate the overall performance of the developed system using different classes of texture images (ceramic tiles, glass products, fabrics and other);

(7) To discuss other non-standard texture defect detection methods with respect to the research carried out.

Research methods and software

This research is based on matrix calculations, methods of discrete wavelet analysis and mathematical (statistical) tools (parameter estimates, statistical hypotheses).

Experiments were carried out in *Matlab R2014a* environment.

Novelty of the research

This dissertation proposes several novel solutions for effectively implementing the texture defect detection system in the spectral discrete wavelet domain. These are:

(1) the proposed texture defect detection technique is based on multiple image scanning; the known methods found in literature are limited to onetime image (or its wavelet spectrum, if wavelet transforms are applied) run-through. Multiple image scanning allows forming a multi-valued texture defect detection criterion, when the final decision on the quality of the texture image under processing is made depending on the percentage of unfavourable criterion values.

(2) the task-oriented statistical analysis of specific subsets of Haar wavelet

coefficients of a texture image enhances the implementation of the texture defect detection system (methodology), which can control true-positive and true-negative image classification process, thereby ensuring the flexibility of the system.

(3) the same criteria and principles of analysis are explored for texture defect localization, as previously used for defect detection in texture images.

(4) a novel fast algorithm for computing Haar wavelet spectra of the selected texture image fragments is proposed. The efficiency of the algorithm leans upon the fact that the absolute majority of Haar wavelet coefficients found for the whole texture image are transferred without any changes to the fragmental spectra. This circumference is of particular importance in real-time applications.

Defence statements

(1) The decision about the quality of the test texture image is based on the results of multiple image scanning when a different filter for two-dimensional discrete wavelets is employed for each scan. This ensures a relatively high (83–98 %) accuracy of testing;

(2) The proposed novel algorithm for computing the discrete Haar wavelet spectra of the selected image fragments is 10–30 times faster than the direct procedures for obtaining fragmental spectra of the image;

(3) The detected defects are localized by employing appropriately chosen subsets of the multi-valued texture defect detection criterion;

(4) The results of the experimental analysis obtained by applying the newly developed defect detection and localization system proved the effectiveness and appeal of the proposed solutions.

Practical significance of the research results

The solutions proposed in this dissertation, i.e. image texture analysis by employing two-dimensional filters for discrete wavelets, an original algorithm for computing the Haar spectrum of the selected image fragments, and principles for generating defect detection criterion can be successfully applied not only in defect detection and localization processes but also in other fields related to digital image processing, such as object localization in lattice-structured images, locally progressive image coding, feature extraction, etc.

It should be noted that the proposed defect detection and localization technique allows classifying texture images and localizing the detected defects in real time. This is especially important when it comes to the automated textured surface testing systems.

Approbation of the dissertation results

Six scientific papers on the subject of the dissertation have been published. Four of them have appeared in international journals with citation indices, included in the main list of the International Scientific Institute Database, others –

in conference materials. The research on the subject of the dissertation has been presented at two international and two national conferences.

The structure

The doctoral dissertation consists of an introduction, four main chapters, conclusions, a list of references and scientific publications. The volume of dissertation is 104 pages. It contains 35 figures, 13 tables and 145 references.

1. LITERATURE REVIEW

This dissertation gives an extensive overview of defect detection methods for texture images. Even though the visual techniques employed in defect detection research are very diverse and constantly changing, all the basic methods of analysis can be divided into several main groups, in particular: statistical, spectral, model-based and structural analysis (Karimi et al., 2014; Ngan et al., 2011; Xie, 2008).

Statistical approach methods analyse the spatial distribution of the pixel values. The main purpose of this analysis is to detect changes in the various statistical parameters of the image regions. Many statistical texture features have been proposed, ranging from first order statistics to higher order statistics. Amongst them, histogram statistics (mean, standard deviation, variance, median, etc.) (Saeidi et al., 2015; Yuan et al., 2015), co-occurrence matrices (Hu et al., 2011; Raheja et al., 2013), autocorrelation function (Tolba, 2012; Hoseini et al., 2013), local binary patterns (Tajeripour et al., 2014; Song et al., 2013), principal and independent component analysis (Chen et al., 2011; Tsai et al., 2008) and Weibul distribution (Timm et al., 2011) have been applied to visual inspection.

In the structural approach, texture is characterised by texture primitives or texture elements and the spatial arrangement of these primitives. Thus, the primary goals of the approach are, firstly, to extract texture primitives and, secondly, to model or generalise the spatial placement rules. The main disadvantages of these methods are that they work well only with regular textures. This approach widely uses morphological operations (Elbehiery et al., 2007; Mak et al., 2009) and edge detection techniques (Najafabadi et al., 2011; Sham et al., 2008) for defect detection.

Filtering technologies are spectral analysis methods for texture surfaces which are analysed as spectral coefficient sets. Image components representing spectral features of desired frequency are extracted based on the energy of the transformation. These features show low sensitivity to noise, so it is often used for defect detection tasks. The main methods for such techniques are Fourier analysis (Chen et al., 2013; Tsai et al., 2012), Gabor filters (Hu, 2015; Mak et al., 2008) or discrete wavelet transforms (Ngan et al., 2011; Guan et al., 2014).

A different approach to texture analysis is based on trying to determine the analytical model of the image using the model-based methods. Such models are

built on the assumption that each pixel in the image is a weighted average of the intensities of the neighbouring pixels. The model parameters define the texture. These methods include texture analysis, which is based on the application of autoregressive models (Bu et al., 2010; Chuang et al., 2009), Markov random fields (Hadizadeh et al., 2008; Hu et al., 2014) and the fractal model (Bu et al., 2008, 2009; Hanmandlu et al., 2015).

The majority of defect detection methods found in literature are adapted to process one type of texture surfaces. They are oriented to detect specific defects such as slub (Liu et al., 2008), pincher (Chuang et al., 2009), knots (Hu et al., 2011) and colour tonality (Xie et al., 2006). However, at present there is a growing need to develop more flexible defect detection systems suitable for processing several types of texture surfaces. For instance, Kwon et al. (2015) indicates that seven different classes of texture images have been tested using Variance of Variance (VOV) profiles applied to the random forest-based machine learning algorithm. An article by Yuan et al. (2015) describes a modified Otsu method with the weight function which can be used to detect defects on texture surfaces, such as wood, fabric, metal, rail images, etc. Hu et al. (2014) propose a wavelet-domain hidden Markov tree (HMT) model to process such surfaces like textile fabric, woven wool, leather and sandpaper.

The literature analysis shows that there is a lack of research concerning the defect detection for various types of textures. Nor are there any generalized algorithms for detecting different types of defects. Finally, the literature review shows that hybrid methods would be useful for industrial applications. Therefore, the visual method based on discrete wavelet transforms and the statistical approach can be developed in the context of texture defect detection. Due to this reason, this dissertation proposes several approaches for analysing images of different texture types.

2. GENERATING THE DEFECT DETECTION AND LOCALIZATION TECHNIQUE FOR TEXTURE IMAGES

The approach proposed in this dissertation is based on the discrete Haar wavelet transform. This choice has been determined by several factors: firstly, the Haar transform is fully localized in space. This feature allows a more comprehensive and effective usage of the proposed defect detection criterion. Secondly, Haar functions are square-shaped. This is a great advantage when the analysed image is characterised by sharp changes in contrast, which is the case in texture defect detection context.

2.1. Generating and investigating the defect detection technique for texture images

2.1.1. Discrete Haar transform, its features and fast computational algorithms

Each discrete wavelet transform (DWT) can be realized iteratively by applying coefficients of the scaling function (low frequency filter) and the wavelet function (high frequency filter).

Let us take an initial data vector (one-dimensional image) $X = (X(0)\ \ X(1)\ \ ...\ \ X(N-1))^T$ $(N = 2^n,\ n \in \mathbb{N})$. After the i-th iteration $i \in \{1, 2, ..., n\}$, the intermediate vectors obtained by applying low and high frequency filters shall be defined as follows:

$$S^{(i)} = \left(s_0^{(i)}\ s_1^{(i)}\ ...\ s_{2^{n-i}-1}^{(i)}\right)^T, \tag{1}$$

$$D^{(i)} = \left(d_0^{(i)}\ d_1^{(i)}\ ...\ d_{2^{n-i}-1}^{(i)}\right)^T; \tag{2}$$

here $S^{(0)} = \left(s_0^{(0)}\ s_1^{(0)}\ ...\ s_{2^{n-i}-1}^{(0)}\right)^T = X$.

The DWT spectrum Y for data vector $X = (X(0)\ \ X(1)\ \ ...\ \ X(N-1))^T$ is obtained after n iterations and is specified as follows:

$$Y = \left(s_0^{(n)}\ d_0^{(n)}\ d_0^{(n-1)}\ d_1^{(n-1)}\ d_0^{(n-2)} d_1^{(n-2)}\ ...\ d_0^{(1)}\ d_1^{(1)}\ ...\ d_{N/2-1}^{(1)}\right)^T. \tag{3}$$

In general, the computational procedure for the DWT spectrum Y can be implemented by using the DWT matrix T_{DWT}:

$$T_{DWT}\,(n-i+1) \cdot S^{(i-1)} = \begin{pmatrix} S^{(i)} \\ D^{(i)} \end{pmatrix}, \tag{4}$$

where $S^{(n)} = \left(s_0^{(n)}\right)$ and $D^{(n)} = \left(d_0^{(n)}\right)$.

The structure of matrix $T_{DWT} = T_{DWT}\,(n-i+1), i \in \{1, 2, ..., n\}$, depends on the specific DWT scaling and wavelet functions, i.e. on the applied filter coefficients. For example, the discrete Haar transform (HT) is characterized by the following sets of coefficients: scaling function (low frequency filter) – $h_0 = 1/\sqrt{2}$ and $h_1 = 1/\sqrt{2}$, and wavelet function (high frequency filter) – $g_0 = h_1 = 1/\sqrt{2}$ and $g_1 = -h_0 = -1/\sqrt{2}$. Thus, the HT matrix is as follows:

$$T_{HT}(n) = \frac{1}{\sqrt{2}} \begin{pmatrix} 1 & 1 & 0 & 0 & 0 & \cdots & 0 & 0 \\ 0 & 0 & 1 & 1 & 0 & \cdots & 0 & 0 \\ \cdots & \cdots & \cdots & \cdots & \cdots & \cdots & \cdots & \cdots \\ 0 & 0 & 0 & 0 & 0 & \cdots & 1 & 1 \\ 1 & -1 & 0 & 0 & 0 & \cdots & 0 & 0 \\ 0 & 0 & 1 & -1 & 0 & \cdots & 0 & 0 \\ \cdots & \cdots & \cdots & \cdots & \cdots & \cdots & \cdots & \cdots \\ 0 & 0 & 0 & 0 & 0 & \cdots & 1 & -1 \end{pmatrix}, \tag{5}$$

where $n = 1, 2, \ldots$.

To find the HT spectrum, usually a fast calculation algorithm is applied which can be defined by the following expressions (Valantinas et al., 2013):

$$s_k^{(i)} = h_0 \cdot s_{2k}^{(i-1)} + h_1 \cdot s_{2k+1}^{(i-1)} = \frac{1}{\sqrt{2}}\left(s_{2k}^{(i-1)} + s_{2k+1}^{(i-1)}\right), \tag{6}$$

$$d_k^{(i)} = g_0 \cdot s_{2k}^{(i-1)} + g_1 \cdot s_{2k+1}^{(i-1)} = \frac{1}{\sqrt{2}}\left(s_{2k}^{(i-1)} - s_{2k+1}^{(i-1)}\right), \tag{7}$$

for all $k = 0, 1, \ldots, 2^{n-i} - 1$, $i \in \{1, 2, \ldots, n\}$.

It should be noted that each numerical value of the HT spectral coefficient is specified by a certain (strictly-fixed) subset with data vector X elements.

It is evident that the numerical values of the spectral coefficients obtained during each iteration are unambiguously specified by non-overlapping subsets of data vectors X, whose union corresponds to X. This situation in different contexts is defined as a feature of the full HT localization in space.

HT can be easily generalized for two-dimensional images. Practical realisation of the two-dimensional HT is entered into the $2N$-th application of the one-dimensional HT: firstly, one-dimensional data vectors $[X(m_1, m_2)]$ at fixed index m_2 values ($m_2 \in \{0, 1, \ldots, N-1\}$) are processed and an intermediate data array $[Y(k_1, m_2)]$ is obtained; further, rows of intermediate data array are processed at fixed k_1 values ($k_1 \in \{0, 1, \ldots, N-1\}$). The last step provides a two-dimensional discrete HT spectrum $[Y(k_1, k_2)]$ of the initial image $[X(m_1, m_2)]$. The order of processing rows and columns does not affect the final result.

2.1.2. Generating the defect detection criterion for texture images

2.1.2.1. Partitioning the discrete Haar spectrum in the texture images

Let $X = [X(m_1, m_2)]$ be a two-dimensional grey-scale digital $N \times N$ ($N = 2^n$, $n \in \mathbb{N}$) image and $Y = [Y(k_1, k_2)]$ be its discrete HT spectrum.

The new defect detection system for texture images has been developed and implemented in the Haar wavelet domain considering the following two factors:

(1) the numerical value of the Haar wavelet coefficient $Y(k_1, k_2)$ ($k_1, k_2 \in \{1, 2, \ldots, N-1\}$; $k_s = 2^{n-i_s} + j_s$, $i_s \in \{1, 2, \ldots, n\}$, $j_s \in \{0, 1, \ldots, 2^{n-i_s} - 1\}$, $i_s = 1, 2$) is uniquely specified by the image block $X^{(k_1, k_2)}$ of size $2^{i_1} \times 2^{i_2}$,

with $X^{(k_1,k_2)}(0,0) = X(2^{i_1}j_1, \ 2^{i_2}j_2)$;

(2) the discrete HT spectrum Y of X can be partitioned into a finite number of non-intersecting subsets (regions) $\Re(0,0)$, $\Re(i_1,0)$, $\Re(0,i_2)$ and $\Re(i_1,i_2)$ $(i_1,i_2 = 1,2,...,n)$, containing 1, 2^{n-i_1}, 2^{n-i_2} and $2^{2n-i_1-i_2}$ Haar wavelet coefficients, respectively (Fig. 2.1). The numerical values of all Haar wavelet coefficients falling into a particular region $\Re(i_1,i_2)$ $(i_1,i_2 \in \{0,1,...,n\})$ are specified by non-overlapping image blocks covering the whole image X.
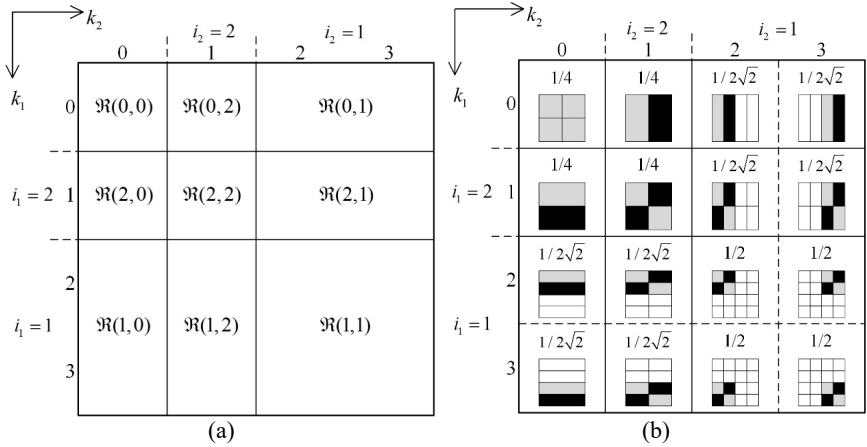
Fig. 2.1. Discrete Haar wavelet transform ($N = 4$): (a) Regions of Haar spectral coefficients characterized by the same computational scheme; (b) Evaluating Haar spectral coefficients (pixel values falling into the black area of the image block are subtracted from those falling into the respective grey area; the algebraic sum then is multiplied by the scalar located above)

2.1.2.2. Statistical analysis of the discrete Haar spectrum regions

A set of defect-free texture images $\{X_1, X_2, ..., X_r\} \subset T$ (T stands for the total population of all defect-free images) which consists of $N \times N$ ($N = 2^n$, $n \in \mathbb{N}$) sized images is analysed. $\{Y_1, Y_2, ..., Y_r\}$ represents the set of the corresponding HT spectra.

The defect detection criterion for texture images is developed on the basis of the following steps:

1) Computation of the averaged spectral coefficient values for the HT spectra Y_s ($s = 1,2,..,r$) regions $\Re_s(0,0)$, $\Re_s(i_1,0)$, $\Re_s(0,i_2)$ and $\Re_s(i_1,i_2)$ $(i_1,i_2 \in \{1,2,...,n\})$, i.e.:

$$\bar{Y}_s(0,0) = |Y_s(0,0)|, \tag{8}$$

$$\bar{Y}_s(i_1, 0) = \frac{1}{2^{2n-i_1}} \sum_{j_1=0}^{2^{n-i_1}-1} |Y_s(k_1, 0)|, \tag{9}$$

$$\bar{Y}_s(0, i_2) = \frac{1}{2^{2n-i_2}} \sum_{j_2=0}^{2^{n-i_2}-1} |Y_s(0, k_2)|, \tag{10}$$

$$\bar{Y}_s(i_1, i_2) = \frac{1}{2^{2n-i_1-i_2}} \sum_{j_2=0}^{2^{n-i_2}-1} \sum_{j_1=0}^{2^{n-i_1}-1} |Y_s(k_1, k_2)|; \tag{11}$$

2) For each region $\Re(0,0)$, $\Re(i_1, 0)$, $\Re(0, i_2)$ and $\Re(i_1, i_2)$ $(i_1, i_2 \in \{1, 2, \dots, n\})$ the following simple samples are provided:

$$\left(\bar{Y}_1(0,0), \ \bar{Y}_2(0,0), \dots, \ \bar{Y}_r(0,0)\right), \tag{12}$$
$$\left(\bar{Y}_1(i_1, 0), \ \bar{Y}_2(i_1, 0), \dots, \ \bar{Y}_r(i_1, 0)\right), \tag{13}$$
$$\left(\bar{Y}_1(0, i_2), \ \bar{Y}_2(0, i_2), \dots, \ \bar{Y}_r(0, i_2)\right), \tag{14}$$
$$\left(\bar{Y}_1(i_1, i_2), \ \bar{Y}_2(i_1, i_2), \dots, \ \bar{Y}_r(i_1, i_2)\right); \tag{15}$$

3) The generated samples are analysed statistically to test the non-parametric statistical hypothesis on the distribution of the mean values (random variables) $\bar{Y}$ of the spectral coefficient representing the specific region and relating to the total population T. A compatibility criterion (statistics) χ^2 is used to test the hypothesis;

4) The so-called σ-intervals $I_p(0,0)$, $I_p(i_1, 0)$, $I_p(0, i_2)$ and $I_p(i_1, i_2)$ with fixed (selected) probability p $(p \in [0.5; 0.99])$ are generated for all regions $\Re(0,0)$, $\Re(i_1, 0)$, $\Re(0, i_2)$, and $\Re(i_1, i_2)$ $(i_1, i_2 \in \{1, 2, \dots, n\})$, depending on the detected distribution, namely:

(1) In the case of normal distribution $\bar{Y} \sim N(m, \sigma)$,

$$I_p = I_p(i_1, i_2) = (m - t \cdot \sigma, \ m + t \cdot \sigma), \tag{16}$$

where $t = \Psi^{-1}(p/2)$ and $\Psi(x) = \frac{1}{\sqrt{2\pi}} \int_0^x e^{-t^2/2} dt$ is the Laplace function; in other words, $P\{\bar{Y} \in I_p\} = p$;

(2) In the case of log-normal distribution $\bar{Y} \sim \ln N(m, \sigma)$,

$$I_p = I_p(i_1, i_2) = \left(\frac{m}{\sigma^t}, \ m \cdot \sigma^t\right), \tag{17}$$

where $t = \Psi^{-1}(p/2)$;

(3) In the case of exponential distribution $\bar{Y} \sim E(\lambda)$,

$$I_p = I_p(i_1, i_2) = [0, \ t \cdot \sigma), \tag{18}$$

where $t = -\ln(1-p)$ and $\sigma = 1/\lambda$.

In this way, a multi-valued defect detection criterion for texture images $N{\times}N$ ($N = 2^n$, $n \in \mathbb{N}$) is developed. The flexibility of the criterion and thereby the possibility of adapting the proposed defect detection technique for different classes of texture images is guaranteed by the selected parameter (probability) ($p \in [0{,}5; 0{,}99]$).

The tested image X_{test} is assumed to be defect-free, if not less than $p(n+1)^2$ of all the averages from the set $\{\bar{Y}_{test}(0,0),\ \bar{Y}_{test}(i_1,0),\ \bar{Y}_{test}(0,i_2),$ $\bar{Y}_{test}(i_1,i_2)|\ \ i_1,i_2 \in \{1,2,\dots,n\}\}$ fall into the corresponding σ-intervals I_p. Otherwise, the image X_{test} is considered to be defective.

Obviously, in constructing σ-intervals for $\Re(i_1,i_2)$ ($i_1,i_2 \in \{0,1,2,\dots,n\}$), we can state statistical hypotheses (with an acceptable significance level) about the appropriateness of any other probability distribution, and construct respective σ-intervals. But, if no suitable distributions are found, the criteria for $\Re(i_1,i_2)$ ($i_1,i_2 \in \{0,1,2,\dots,n\}$) are formed using the minimal and maximal average values, i.e. $I_p = I_p(i_1,i_2) = [\bar{Y}_{min}, \bar{Y}_{max}]$. In this case, the interval is independent on the parameter p, what lowers the flexibility of the entire system.

Undoubtedly, in constructing texture defect detection criteria higher-order statistics (variance, kurtosis, higher-order moments, etc.) can be employed. Unfortunately, the usage of higher-order statistics considerably increases the number of regions with intervals of type $[\bar{Y}_{min}, \bar{Y}_{max}]$. Also, experimental studies have shown that the exploration of higher-order statistics (variance and kurtosis) does not meet the requirements of texture defect classification.

2.2. Organization of defect localization in texture images

Let us consider a defective texture image $X_{def} = [X_{def}(m_1, m_2)]$ with dimensions of $N{\times}N$ ($N = 2^n$, $n \in \mathbb{N}$) and its discrete HT spectrum $Y_{def} = [Y_{def}(k_1, k_2)]$. In order to localize the defect, the image X_{def} is partitioned into a finite number of the same size $2^m{\times}2^m$ ($m \in \{n-1,\ n-2,\dots\}$) non-overlapping fragments $X^{(k_1,k_2)}$ ($k_1, k_2 \in \{2^{n-m}, 2^{n-m}+1,\dots,2^{n-m+1}-1\}$; Section 2.1.2.1). The discrete HT spectra $Y^{(k_1,k_2)} = [Y^{(k_1,k_2)}(u_1,u_2)]$ ($u_1, u_2 = 0,1,\dots,2^m-1$) of the latter fragments are obtained by employing the HT spectrum Y_{def} of the whole image X_{def}.

The transition from the HT spectrum Y_{def} for the image X_{def} to the HT spectrum of the image fragment $X^{(k_1,k_2)}$ is realized by applying a newly developed fast algorithm (Valantinas et al., 2013), namely:

1) The following sets are generated:

$$S_V = \{\alpha_0, \alpha_1, \dots, \alpha_{n-m}\}, \tag{19}$$
$$S_H = \{\beta_0, \beta_1, \dots, \beta_{n-m}\}, \tag{20}$$

$$\mathfrak{I}_1 = \{k_1\} \cup \bigcup_{q=1}^{m-1} \mathfrak{I}_1(q), \quad \mathfrak{I}_1(q) = \{2^q k_1, 2^q k_1 + 1, \dots, 2^q(k_1 + 1) - 1\}, \quad (21)$$

$$\mathfrak{I}_2 = \{k_2\} \cup \bigcup_{q=1}^{m-1} \mathfrak{I}_2(q), \quad \mathfrak{I}_2(q) = \{2^q k_2, 2^q k_2 + 1, \dots, 2^q(k_2 + 1) - 1\}; \quad (22)$$

here: $\alpha_0 = k_1$, $\alpha_s = \lfloor \alpha_{s-1}/2 \rfloor$, $s = 1, 2, \dots, n - m$, and $\beta_0 = k_2$, $\beta_t = \lfloor \beta_{t-1}/2 \rfloor$, $t = 1, 2, \dots, n - m$;

2) The HT spectral coefficients $Y^{(k_1,k_2)}(0,0)$, $Y^{(k_1,k_2)}(u_1, 0)$ and $Y^{(k_1,k_2)}(0, u_2)$ $(u_1, u_2 = 1, 2, \dots, 2^m - 1)$ for the fragment $X^{(k_1,k_2)}$ are found by the following expressions:

$$Y^{(k_1,k_2)}(0,0) = \frac{1}{2^{n-m}} Y_{def}(0,0) + \frac{1}{\sqrt{2^{n-m}}} \sum_{s=1}^{n-m} \frac{(-1)^{\alpha_{s-1}}}{\sqrt{2^s}} \cdot Y_{def}(\alpha_s, 0)$$

$$+ \frac{1}{\sqrt{2^{n-m}}} \sum_{t=1}^{n-m} \frac{(-1)^{\beta_{t-1}}}{\sqrt{2^t}} \cdot Y_{def}(0, \beta_t) + \sum_{s,t=1}^{n-m} \frac{(-1)^{\alpha_{s-1}+\beta_{t-1}}}{\sqrt{2^{s+t}}} \cdot Y_{def}(\alpha_s, \beta_t), \quad (23)$$

$$Y^{(k_1,k_2)}(u_1, 0) = \frac{1}{\sqrt{2^{n-m}}} Y_{def}(k_1^*, 0) + \sum_{t=1}^{n-m} \frac{(-1)^{\beta_{t-1}}}{\sqrt{2^t}} \cdot Y_{def}(k_1^*, \beta_t), \quad (24)$$

$$Y^{(k_1,k_2)}(0, u_2) = \frac{1}{\sqrt{2^{n-m}}} Y_{def}(0, k_2^*) + \sum_{s=1}^{n-m} \frac{(-1)^{\alpha_{s-1}}}{\sqrt{2^s}} \cdot Y_{def}(\alpha_s, k_2^*), \quad (25)$$

with all the $u_1, u_2 = 1, 2, \dots, 2^m - 1$; k_1^*, k_2^* are respectively u_1-th and u_2-th elements of sets $\mathfrak{I}_1$ and $\mathfrak{I}_2$ (the numbering of elements in sets $\mathfrak{I}_1$ and $\mathfrak{I}_2$ starts from one);

3) The remaining HT spectral coefficients $Y^{(k_1,k_2)}(u_1, u_2)$ $(n_1, n_2 = 1, 2, \dots, 2^m - 1)$ for fragment $X^{(k_1,k_2)}$ are simply selected from the spectrum Y_{def}, i.e. $Y^{(k_1,k_2)}(u_1, u_2) = Y_{def}(k_1^*, k_2^*)$; here k_1^* and k_2^* are respectively u_1-th and u_2-th elements of sets $\mathfrak{I}_1$ and $\mathfrak{I}_2$ (the numbering of elements in sets $\mathfrak{I}_1$ and $\mathfrak{I}_2$ starts from one).

According to the described fast algorithm, once the discrete HT spectrum $Y^{(k_1,k_2)}$ $(k_1, k_2 \in \{2^{n-m}, 2^{n-m} + 1, \dots, 2^{n-m+1} - 1\})$ for image's X_{def} fragment $X^{(k_1,k_2)}$ is obtained, further image analysis is carried out. The HT spectrum $Y^{(k_1,k_2)}$ is divided into non-overlapping regions (Section 2.1.2) $\mathfrak{R}^{(k_1,k_2)}(0,0)$, $\mathfrak{R}^{(k_1,k_2)}(i_1, 0)$, $\mathfrak{R}^{(k_1,k_2)}(0, i_2)$ and $\mathfrak{R}^{(k_1,k_2)}(i_1, i_2)$ $(i_1, i_2 \in \{1, 2, \dots, m\})$, for which the following conclusions are correct (provided that the processed image X_{def} represents the class of images characterized by smooth texture and quite fine pattern):

– The HT coefficient $\left|Y^{(k_1,k_2)}(0,0)\right|$ for region $\mathfrak{R}^{(k_1,k_2)}(0,0)$ with the multiplier 2^{n-m} falls into (or, escapes) the previously determined interval $I_p = I_p(0,0)$ (Section 2.1.2.2);

– Averages of spectral coefficients $\bar{Y}^{(k_1,k_2)}(i_1,0)$ and $\bar{Y}^{(k_1,k_2)}(0,i_2)$ $(i_1, i_2 \in \{1,2,\dots,m\})$, for regions $\mathfrak{R}^{(k_1,k_2)}(i_1,0)$ and $\mathfrak{R}^{(k_1,k_2)}(0,i_2)$, with the multiplier $(\sqrt{2})^{n-m}$ belong (or, do not belong) to the interval $I_p(i_1,0)$ and $I_p(0,i_2)$ of the criterion;

– Averages $\bar{Y}^{(k_1,k_2)}(i_1,i_2)$ $(i_1, i_2 \in \{1,2,\dots,m\})$ of the spectral coefficients for the regions $\mathfrak{R}^{(k_1,k_2)}(i_1,i_2)$ fall into (or, escape) $I_p = I_p(i_1,i_2)$.

Thus, with a fixed probability p, the image fragment $X^{(k_1,k_2)}$ is recognized as defect-free, provided that at least $p(m+1)^2$ average dependency for corresponding σ-intervals is met. In other words, for defect localization, the same texture defect detection criterion can be explored. An illustration of regions applied to defect localization is provided in Fig. 2.2.

It should be noted that in cases when the requirements for texture are not met (smoothness, fine print, etc.), the texture defect detection criteria (in the context of defect localization) should be developed individually for every image fragment $X^{(k_1,k_2)}$ $(k_1, k_2 \in \{2^{n-m}, 2^{n-m}+1, \dots, 2^{n-m+1}-1\})$, based on analogous considerations for the whole texture image (Section 2.1.2.).

When it comes to the usage of higher order DWT in the texture defect localization process, it has been observed that fast transition from DWT spectrum of the whole texture image to fragmental spectra of image blocks is no longer possible, unless some special decorrelation procedures are applied to the DWT in use (Valantinas et al., 2013).

$I_p(0,0)$	$I_p(0,n)$	$I_p(0,n-1)$	...	$I_p(0,m)$	...	$I_p(0,2)$	$I_p(0,1)$
$I_p(n,0)$	$I_p(n,n)$	$I_p(n,n-1)$	...	$I_p(n,m)$	...	$I_p(n,2)$	$I_p(n,1)$
$I_p(n-1,0)$	$I_p(n-1,n)$	$I_p(n-1,n-1)$	...	$I_p(n-1,m)$	...	$I_p(n-1,2)$	$I_p(n-1,1)$
$\vdots$	$\vdots$	$\vdots$	$\ddots$	$\vdots$	$\vdots$	$\vdots$	$\vdots$
$I_p(m,0)$	$I_p(m,n)$	$I_p(m,n-1)$	...	$I_p(m,m)$	...	$I_p(m,2)$	$I_p(m,1)$
$\vdots$	$\vdots$	$\vdots$	$\vdots$	$\vdots$	$\ddots$	$\vdots$	$\vdots$
$I_p(2,0)$	$I_p(2,n)$	$I_p(2,n-1)$	...	$I_p(2,m)$	...	$I_p(2,2)$	$I_p(2,1)$
$I_p(1,0)$	$I_p(1,n)$	$I_p(1,n-1)$	...	$I_p(1,m)$	...	$I_p(1,2)$	$I_p(1,1)$

Fig. 2.2. Defect detection criterion for image $2^n \times 2^n$; for the analysis of $2^m \times 2^m$ image blocks only the white coloured zones with corresponding multipliers are used

2.3. Chapter conclusions

The discrete Haar wavelet transform allows developing a very effective defect detection technique for texture images. Due to full localization in space, this transform accumulates image features in various levels of image detailing.

A texture defect detection technique (system) based on statistical image analysis in the spectral discrete wavelet domain is proposed. The system is controllable and flexible with respect to the defect, i.e. it gives an opportunity to select an appropriate value of a parameter (probability) p which could reduce the number of incorrectly recognized texture images.

The developed defect detection technique scans the image for $(n + 1)^2$ times, i.e. the defect detection criterion is based on multiple image scanning, which suggests that the results of the analysis are meticulous and correspond with the information compiled in the image.

The proposed system allows analysing the target regions by paying attention to the specific image texture. Despite the fact that some of the regions are rejected in this way, the entire image information is retained.

The described novel technique for defect localization is characterized by several original ideas. Firstly, a newly developed fast computational algorithm for the fragment HT spectrum is applied: the majority of spectral coefficients are simply selected from the HT spectrum of the whole image. Secondly, under certain conditions, this technique does not require a criterion recalculation. This dissertation demonstrates that averages of HT spectral coefficients for regions $\Re(i_1, i_2)$, when switching from the image $2^n \times 2^n$ to fragments $2^m \times 2^m$, differ in a specified multiplier (with a minor error ε).

3. REALISATION OF THE DEFECT DETECTION AND LOCALIZATION TECHNIQUE FOR TEXTURE IMAGES

3.1. The organization of the experiment

In this part of the research, the following classes of texture images are employed to assess the overall performance of the defect detection and localization technique: ceramic tiles, glass sheets and fabric scraps. All sets of texture images were obtained from the major Lithuanian industrial companies. Examples of the investigated texture images are provided in Fig. 3.1. Data sets of the first two classes are compiled of 100 defect-free and 100 defective texture images. The set of fabric scraps is compiled of 100 defect-free and 60 defective images. All the analysed images are characterised by a grey light intensity scale, and their size is 256×256 pixels.

The general technique for texture defect detection proposed for grey-scale images is presented in Fig. 3.2. The defect detection process comprises six main steps:

1) Obtaining the discrete wavelet spectra (DWT) Y_j $(j = 1, 2, \dots, r)$ for the

selected defect-free texture images X_j $(j = 1, 2, ..., r)$;

2) Partitioning the spectrum Y_j $(j \in \{1, 2, ..., r\})$ into non-overlapping subsets (regions) $\Re(i_1, i_2)$ $(i_1, i_2 = 0, 1, ..., n)$;

3) Statistically analysing the spectral coefficients falling into the region $\Re(i_1, i_2)$ $(i_1, i_2 \in \{0, 1, ..., n\})$;

4) Generating the defect detection criterion (σ-intervals) $I_p = I_p(i_1, i_2)$ $(p \in [0.5; 0.99])$ for all regions $\Re(i_1, i_2)$ $(i_1, i_2 = 0, 1, ..., n)$;

5) Testing the texture image X_{test};

6) Localising the defect in the defective texture image.

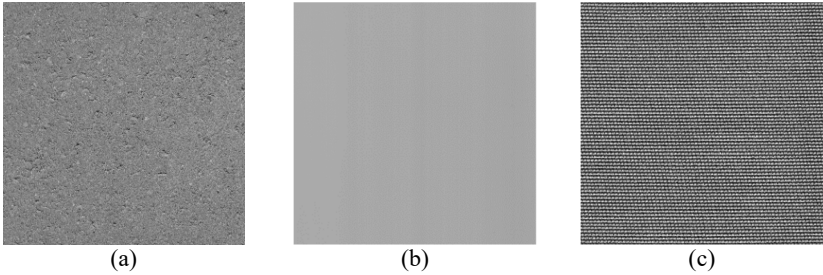(a)   (b)   (c)

Fig. 3.1. Defect-free texture images: (a) ceramic tile; (b) glass sheet; (c) fabric scrap
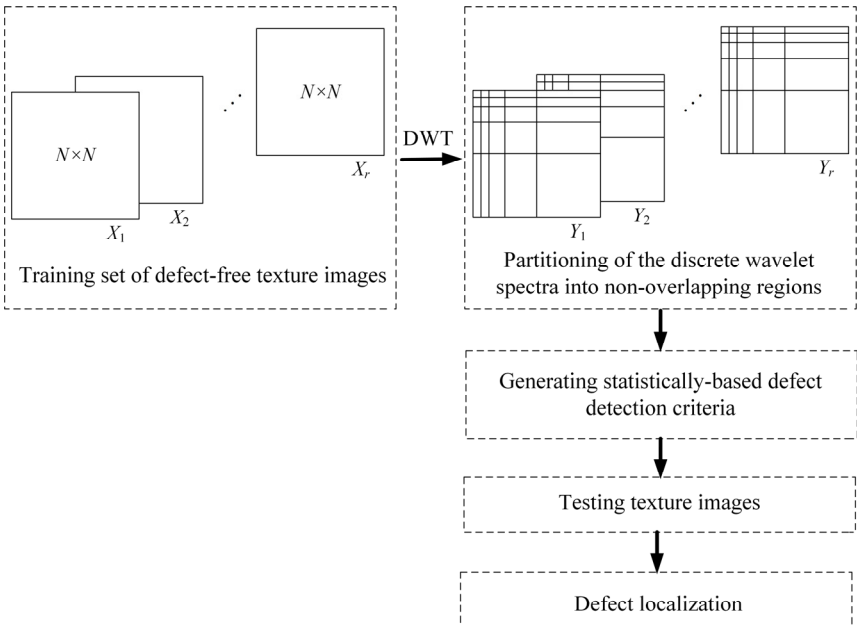

Fig. 3.2. The structural scheme of defect detection and localization in texture images

During the experiment, the defect detection criterion was generated by selecting 50 defect-free images from each class of texture images. The overall performance of the texture defect detection technique was evaluated by conducting five experiments with each group. Each experiment was carried out by randomly selecting 50 defect-free and 50 defective images both from ceramic tiles and glass sheets, and respectively 30 images from the class of fabric scraps.

3.2. Experimental analysis of the texture images

The classification results which were obtained by applying the technique presented in chapter 3.1. They cover all the said five experiments which are presented in Tables 3.1–3.3, where the parameters are as follows: TP (*true positive*) means that the tested defective images are recognized as defective, TN (*true negative*) means that defect-free images are recognized as defect-free, FP (*false positive*) means that defect-free images are recognized as defective, FN (*false negative*) means that defective images are recognized as defect-free.

It is rather evident that the classification results of ceramic tiles (Table 3.1) indicate that the quality of texture images is determined correctly in all five experiments (i.e. a good image is recognized as good, and a bad image is recognized as bad) in more than 92 % of cases, when $p = 0.99$, and in more than 90 % of cases, when $p = 0.95$ and $p = 0.90$. Summarizing all five experiments, it can be stated that defective images are identified correctly, on average, in 98 % of cases, while defect-free images, on average, in 95 % of cases.

Table 3.1. Classification of ceramic tiles

Probability, p		Serial number of the experiment				
		1	2	3	4	5
0.99	TP	100 %	98 %	96 %	98 %	100 %
	FP	2 %	2 %	8 %	4 %	4 %
	TN	98 %	98 %	92 %	96 %	96 %
	FN	0 %	2 %	4 %	2 %	0 %
0.95	TP	100 %	98 %	96 %	98 %	100 %
	FP	2 %	0 %	10 %	4 %	10 %
	TN	98 %	100 %	90 %	96 %	90 %
	FN	0 %	2 %	4 %	2 %	0 %
0.90	TP	98 %	90 %	94 %	98 %	100 %
	FP	4 %	4 %	10 %	2 %	6 %
	TN	96 %	96 %	90 %	98 %	94 %
	FN	2 %	10 %	6 %	2 %	0 %

During the analysis of fabric images, their specific texture, i.e. tendency to regularity, was taken into account. It has been noticed that a more suitable analysis for the said images should be performed without incorporating regions of the multi-aspect criterion, which analyse the neighbouring pixels of the texture image. The following research results for this class were obtained by applying the

criterion $\{I_p = I_p(i_1, i_2)\}$ ($i_1, i_2 \in \{0, 2, 3, 4, 5, 6, 7, 8\}$). The research presented in Table 3.2 reveals that the best classification results are obtained when probability p equals 0.975. Then the success rate of texture defect detection (TP+TN)/(TP+FN+TN+FP) is equal to 0.94. When $p = 0.95$, the success rate is 0.922 and has a tendency to decrease, with decreasing values of p.

Table 3.2. Classification of fabric products

Probability, p		Serial number of the experiment				
		1	2	3	4	5
0.99	TP	97 %	93 %	93 %	97 %	93 %
	FP	30 %	33 %	23 %	23 %	30 %
	TN	70 %	67 %	77 %	77 %	70 %
	FN	3 %	7 %	7 %	3 %	7 %
0.975	TP	93 %	90 %	90 %	93 %	90 %
	FP	3 %	3 %	3 %	0 %	7 %
	TN	97 %	97 %	97 %	100 %	93 %
	FN	7 %	10 %	10 %	7 %	10 %
0.95	TP	90 %	90 %	87 %	87 %	87 %
	FP	3 %	3 %	3 %	3 %	7 %
	TN	97 %	97 %	97 %	97 %	93 %
	FN	10 %	10 %	13 %	13 %	13 %

Experimental analysis of glass sheets (Table 3.3) has shown that this class is less sensitive to changes in probability p. This can be explained by the fact that only very small and minor defects (such as scratches) are ignored, while all the others are recognized.

Table 3.3. Classification of glass products

Probability, p		Serial number of the experiment				
		1	2	3	4	5
0.99	TP	98 %	96 %	98 %	98 %	100 %
	FP	6 %	0 %	0 %	0 %	0 %
	TN	94 %	100 %	100 %	100 %	100 %
	FN	2 %	4 %	2 %	2 %	0 %
0.95	TP	98 %	96 %	98 %	98 %	100 %
	FP	8 %	6 %	4 %	6 %	6 %
	TN	92 %	94 %	96 %	94 %	94 %
	FN	2 %	4 %	2 %	2 %	0 %
0.90	TP	98 %	96 %	98 %	98 %	100 %
	FP	10 %	8 %	6 %	14 %	12 %
	TN	90 %	92 %	94 %	86 %	88 %
	FN	2 %	4 %	2 %	2 %	0 %

The results of defect localization are presented in Fig. 3.3. In all cases the defective texture image 256×256 was divided into smaller blocks of size 64×64,

and then each block was analysed. Image fragments which failed to satisfy the criterion were assumed to be defective and were marked in a darker colour.
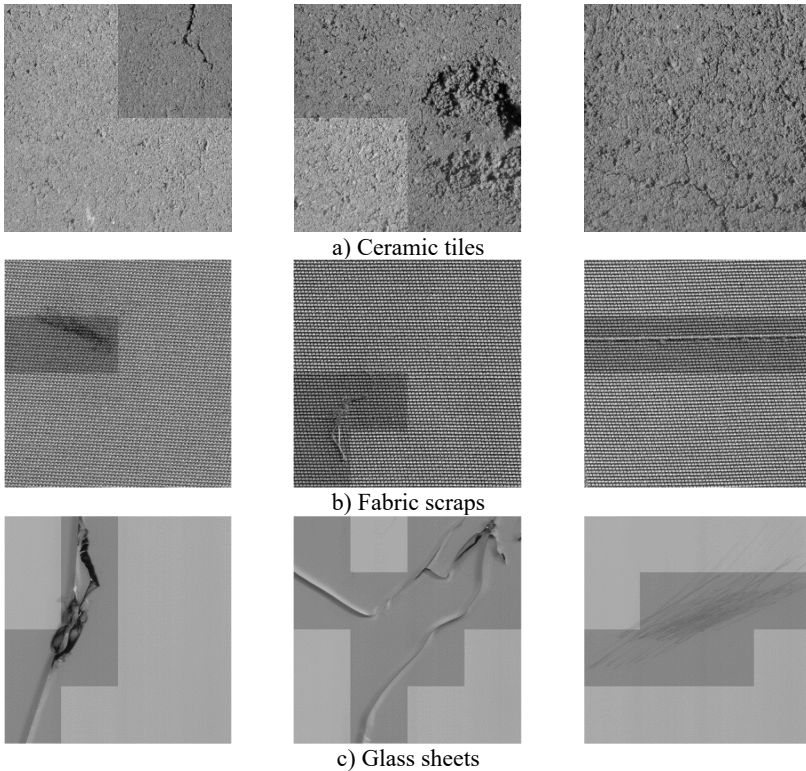
a) Ceramic tiles

b) Fabric scraps

c) Glass sheets

Fig. 3.3. Texture images with localized defects ($p = 0.99$, $m = 6$, $n = 8$)

3.3. Evaluation of the overall performance of the defect detection technique for texture images

In order to evaluate the overall performance of the newly developed texture defect detection technique, three widely used secondary performance parameters of the system were explored, namely: Accuracy (the success rate of texture defect detection) = (TP+TN)/(TP+FN+TN+FP), Sensitivity = TP/(TP+FN) and Specificity = TN/(TN+FP).

The generalized values of the texture defect detection accuracy are provided in Fig. 3.4. The highest obtained rates are: 0.972, for ceramic tiles; 0.984, for glass sheets, when $p = 0.99$; 0.94, for fabric scraps, when $p = 0.975$. Since the accuracy values in all image classes tend to decrease, with the decreasing probability p, in actual applications the p values should be close to 1. Moreover, the average

success rate (accuracy) of the proposed defect detection technique is 0.965.

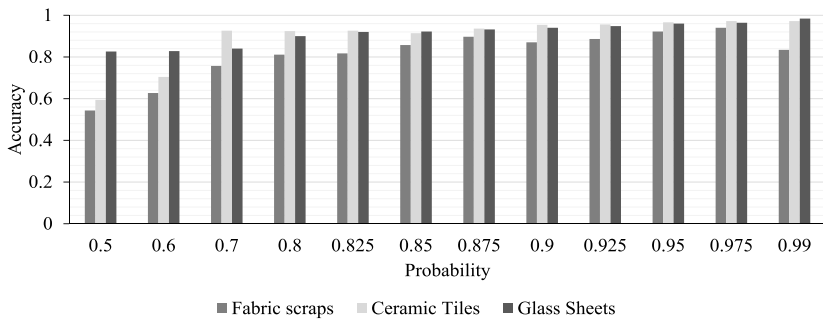**Fig. 3.4.** Dependence of the defect detection accuracy on the system's parameter p
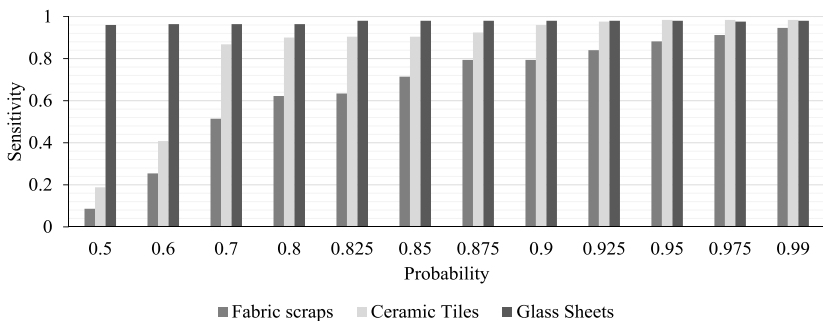

Fig. 3.5. Dependence of the defect detection sensitivity rate on probability p
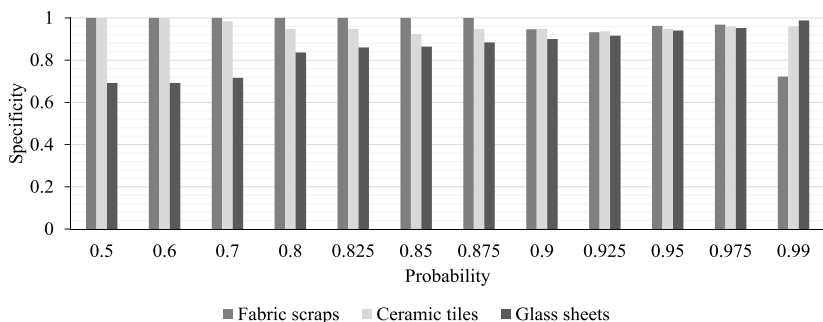

Fig. 3.6. Dependence of the defect detection specificity rate on probability p

Fig. 3.5 and Fig. 3.6 show the dependence of the remaining secondary parameters (sensitivity and specificity) on probability p. The latter parameters are

usually explored to control the risk in the process of texture defect detection: (1) if there is an interest in the selection of highest quality products (fabric scraps, ceramic tiles, glass sheets), i.e. in sorting out all defective products, even at the expense of some defect-free products, the value of p should be chosen in such a way that sensitivity is close to 1 and specificity less than 1; (2) if there is an interest in the second-rate products, the value of p should be fixed so that sensitivity is less than 1 and specificity is close to 1.

For instance, in the case of fabric scraps (Fig. 3.5, Fig. 3.6), for $p = 0.99$: Sensitivity = 0.94 and Specificity = 0.72. It means that 28 % of actually defect-free texture images (however, characterized by negligible defects) are classified as defective. The remaining images classified as defect-free are of the highest quality.

For $p = 0.7$, in the class of ceramic tiles (Fig. 3.5 and Fig. 3.6), Specificity = 1 and Sensitivity = 0.87. Therefore, 13 % of actually defective images are classified as being defect-free. This fact leads to a preparation (classification) of second-rate ceramic tiles.

In the case of glass sheets (Fig. 3.5 and Fig. 3.6), it has been found that Sensitivity = 0.99 for $p = \{0.825, 0.85, 0.875, 0.9, 0.925, 0.95\}$ and Specificity varied from 0.85 to 0.94, respectively. It means that the quality (at the same time percentage) of the classified defect-free images can be controlled, by removing 6 % or more (up to 15 %) of actually defect-free images (perhaps having small defects).

Algorithms proposed by other authors were also employed to evaluate the overall performance of the proposed technique. For comparative analysis, the following methods were selected: 1) the application of VOV profiles with forest-based learning algorithm (Kwon et al., 2015); 2) the co-occurrence matrix (Raheja et al., 2013). These systems were realized in the *Matlab* environment, together with the proposed original method. Table 3.4 provides the results of defect detection accuracy.

All the mentioned facts prove that the proposed defect detection technique is flexible and has a wide range of application possibilities.

Table 3.4. A comparison of the obtained accuracy results for defect detection

	Ceramic tiles	Fabric scraps	Glass sheets	Average accuracy
Proposed method	0.972	0.940	0.984	0.965
VOV features	0.971	0.919	0.918	0.936
Co-occurrence matrix	0.850	0.593	0.866	0.769

3.4. Chapter conclusions

The results of the experimental analysis obtained for three image classes (ceramic tiles, fabric and glass sheets) prove that the proposed defect detection technique is quite versatile and can be applied for analysing various textures.

The research shows that the best classification results for ceramic tiles and

glass sheets are obtained when a full multi-valued criterion is used, whereas the class of fabrics requires applying a task-oriented subset of the criterion (σ-intervals).

A comparative analysis of texture defect detection methods reveals that the newly proposed technique is competitive. A notable advantage is its flexibility which other known and described texture defect detection methods lack.

Since all the texture defect detection systems are designed for real-time application, time consumption also plays an important role. The research shows that the time needed to test a single image, when probability p is fixed, equals 0.028 s and defect localization requires additional 0.04 s. At the same time, a computational complexity of the image defect detection process was assessed, in particular $O(9N^2)$, when $N \times N$ stands for dimensions of the texture image.

4. APPLICATION OF IMAGE SMOOTHNESS AND SIMILARITY ESTIMATES TO THE PROCESS OF TEXTURE DEFECT DETECTION

The concepts of image smoothness and image similarity are very common in digital image processing (fractal image coding, filtering, synthesis and so on). Incidentally, these concepts have been explored in the ball bearing failure diagnostics (Vaideliene et al., 2015), where the bearing fault, bearing inner race and outer race faults were analysed. It was found out that the image smoothness and similarity estimates might reduce computational tolerance in the signal analysis systems. On this basis, experiments were done to employ the image smoothness estimate in the texture image quality analysis as a useful parameter of visual features.

4.1. Mathematical interpretation of image smoothness and image similarity

Let us take a grey-scale image $[X(m_1, m_2)]$ $(m_1, m_2 \in \{0, 1, \dots, N-1\})$ and its discrete (cosine, Fourier, Walsh, etc.) spectrum $[Y(k_1, k_2)]$. We are making an additional assumption that the basis vectors of the discrete transform (DT), i.e. (DT matrix rows) are arranged by their frequency. Then, the DT coefficient array $\{|Y(k_1, k_2)| \big| k_1^2 + k_2^2 \neq 0\}$ can be approximated by a hyperbolic surface:

$$z = z(x, y) = \frac{C}{(x \cdot y)^\alpha}, \qquad (26)$$

where C is a constant and α is defined to be the smoothness parameter for the image $[X(m_1, m_2)]$. To obtain an approximate value (an estimate) of the smoothness parameter α, a fast iterative computational algorithm is applied (Žumbakis et al., 2004), namely:

(1) $\alpha := 0;\ \delta := \delta_{max}$.
(2) Compute: $Y_\Sigma = \sum_{k \in H} |Y(k_1, k_2)|^2$.
(3) Find:

$$Z_Y(\alpha) = \sum_{k \in H} |Y(k_1, k_2)| \cdot A(k_1, k_2, \alpha), \tag{27}$$

$$\tau = \tau(\alpha) = Y_\Sigma - \frac{Z_Y^2(\alpha)}{A(\alpha)}; \tag{28}$$

here: $A(k_1, k_2, \alpha) = 1/(\bar{k}_1 \cdot \bar{k}_2)^\alpha$; $A(\alpha) = \sum_{k \in H} A^2(k_1, k_2, \alpha)$.

(4) If $\tau < \delta$, then $\delta := \tau$. Otherwise, go to step (6).

(5) If $\alpha < \alpha_{max}$, then $\alpha := \alpha + h$ ($h \in (0; 0.1)$), and go back to step (3).

(6) The image smoothness estimate α is obtained.

The dissertation also considers a fragment $U = [U(l_1, l_2)]$ ($l_1, l_2 \in \{0, 1, \ldots, M-1\}$) of the image $[X(m_1, m_2)]$, when the smoothness parameter value (the estimate) of U is α_U. $V = U + \Delta U$ is a new fragment obtained by assigning small inurement ΔU to U and α_V signifies the smoothness parameter value of V.

For assessing the fragmental similarity between U and V, a root mean squared error (metrics) δ is used, i.e.

$$\delta = \delta(U, V) = \left(\frac{1}{M^2} \sum_{l_1, l_2 = 0}^{M-1} \left(V(l_1, l_2) - U(l_1, l_2) \right)^2 \right)^{1/2}. \tag{29}$$

Images U and V are said to be similar if $\delta = \delta(U, V) \leq \delta_0$ (δ_0 being a priori fixed positive number).

It has been proven that small changes in pixel values of the fragment U lead to small changes in the smoothness parameter value α_U, i.e.:

$$(\delta(U, V) = \delta(U, U + \Delta U) \leq \delta_0) \Rightarrow (|\alpha_V - \alpha_U| = |\Delta\alpha_U| \leq \varepsilon_0); \tag{30}$$

here $\varepsilon_0 = \varepsilon(\delta_0)$.

Consequently, the precondition for the similarity of U and V images is defined by the following relationship (the necessary condition for fragmental similarity):

$$(|\alpha_V - \alpha_U| > \varepsilon_0) \Rightarrow (\delta(U, V) > \delta_0). \tag{31}$$

In other words, fragments U and V cannot be similar if their smoothness differ significantly (in terms of the root mean squared error).

4.2. The general texture defect detection technique

To describe the potential capability and effectiveness of application of the fragmental image smoothness and fragmental image similarity to the texture defect detection process, the following considerations are taken into account:

(1) Defect-free texture images $N \times N$ ($N = 2^n$, $n \in \mathbb{N}$) are analysed. During this analysis the defect detection criterion is developed. To be more precise, the

criterion domain is generated in the plane of increments of image smoothness and image similarity. First of all, by averaging all non-overlapping fragments of size $2^l \times 2^l$ $(l < n)$ of the selected defect-free texture image, a reference fragment $U = [U(m_1, m_2)]$ $(m_1, m_2 \in \{0, 1, \ldots, 2^l - 1\})$ is generated and its smoothness parameter α_U is obtained. Then, all the possible fragments V (of double or triple size, in comparison with U) of the remaining defect-free texture images are analysed, i.e. their smoothness estimates α_V are recorded and fragmental similarity for each pairing "$U \leftrightarrow V$" (in terms of is $\delta = \delta(U, V)$) is determined.

(2) By using all the obtained values, i.e. points $\big(|\Delta\alpha_U|, \delta(U, V)\big)$, a "cloud" is generated in the image smoothness and image similarity increments plane for each investigated texture image. The centre $\big(|\Delta\alpha_U|_{vid}, \delta_{vid}(U, V)\big)$ of the "cloud", for each defect-free texture image, is obtained. Next, the maximum and minimum values of the centre coordinates (in the context of all defect-free images) are selected, and a rectangular domain $\mathcal{B}$ of texture defect detection criterion is formed, namely:

$$\mathcal{B} = \{\big(|\Delta\alpha_U|, \delta(U, V)\big) | |\Delta\alpha_U|_{min} \leq |\Delta\alpha_U| \leq |\Delta\alpha_U|_{max},$$
$$\delta_{min}(U, V) \leq \delta(U, V) \leq \delta_{max}(U, V)\}; \tag{32}$$

here: $|\Delta\alpha_U|_{min} = \min\{|\Delta\alpha_U|_{vid}\}$, $|\Delta\alpha_U|_{max} = \max\{|\Delta\alpha_U|_{vid}\}$, $\delta_{min}(U, V) = \min\{\delta_{vid}(U, V)\}$, $\delta_{max}(U, V) = \max\{\delta_{vid}(U, V)\}$.

(3) The same reference fragment U is compared with all the fragments V_{test} (of double or triple size, in comparison with U) of the tested texture image X_{test}. The "cloud" is formed and its centre $\big(|\Delta\alpha_U|_{vid}, \delta_{vid}(U, V_{test})\big)$ is found; here $|\Delta\alpha_U| = \big|\alpha_U - \alpha_{V_{test}}\big|$. An image X_{test} is recognized as defect-free, if this point (centre) falls into the criterion domain $\mathcal{B}$, and as defective otherwise.

4.3. Experimental research

During the experiment, three classes of texture images 256×256 (ceramic tiles, fabric scraps, glass sheets) were investigated. For the reference fragment U of size 16×16 (32×32 or 64×64), all possible pairings with fragments V of size 32×32 (64×64 or 128×128) of the tested image X_{test} were examined.

For all classes, the domains $\mathcal{B}$ of the texture defect detection criteria were generated. For this purpose, 50 defect-free images from each class were used. Fig. 4.1 provides all three cases when the tested image (ceramic tile, fabric scrap, glass sheet) was recognized as defect-free. In all cases, the centre coordinates of the "cloud", i.e. the points $\big(|\Delta\alpha_U|_{vid}, \delta(U, V_{test})\big)$ fell into the respective criterion domain $\mathcal{B}$. Meanwhile, Fig. 4.2 presents the situations when the tested texture images were recognized as defective, as points $\big(\Delta\alpha_U, \delta(U, V_{test})\big)$ escaped the domain $\mathcal{B}$ of the respective criterion.
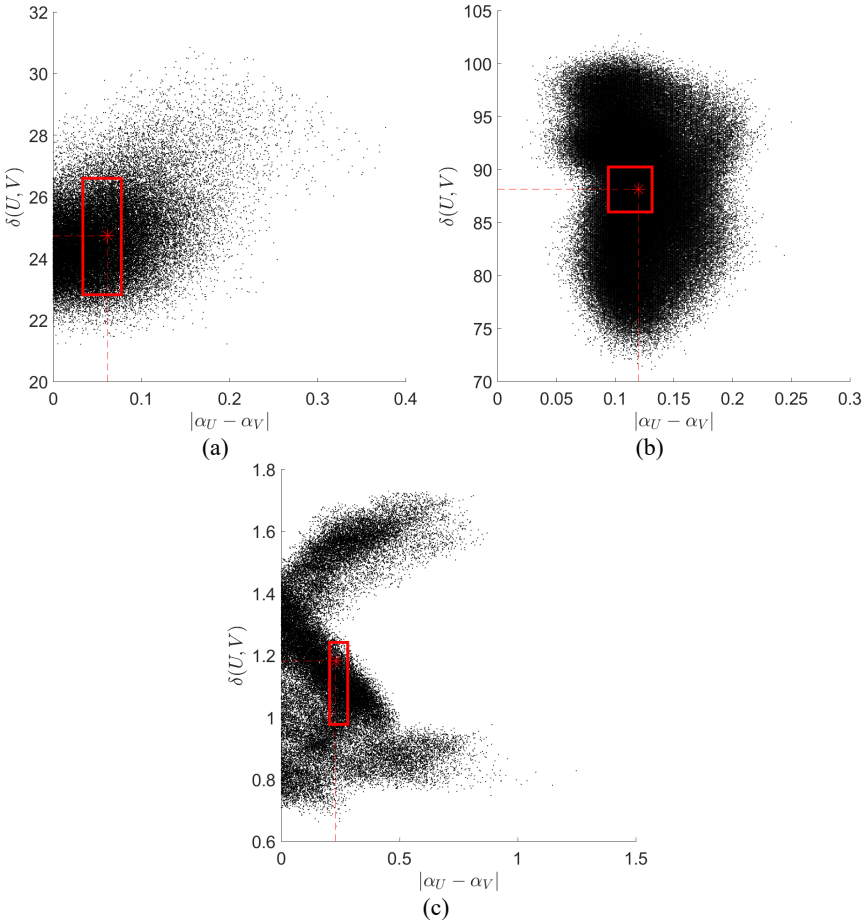
Fig. 4.1. Tested texture image is recognized as defect-free:
(a) ceramic tile; (b) fabric scrap; (c) glass sheet

In connection with this, it is important to emphasize the high concentration of points in the "cloud" (Fig. 4.1 and Fig. 4.2) conditioned, undoubtedly, by the existing strong correlation between image smoothness and image similarity (expression (30)); Section 4.1.) and regularity of the defect-free texture images.

The further stages of the experiment were carried out in the same way as for the statistically-based texture defect detection technique (Section 3). Five experiments were carried out. For each experiment, the defect detection criterion was developed using a half of the compiled defect-free texture images which were selected randomly. All experiments used the same criterion domain $\mathcal{B}$ which was formed of the previously distinguished subset of images (Section 3).
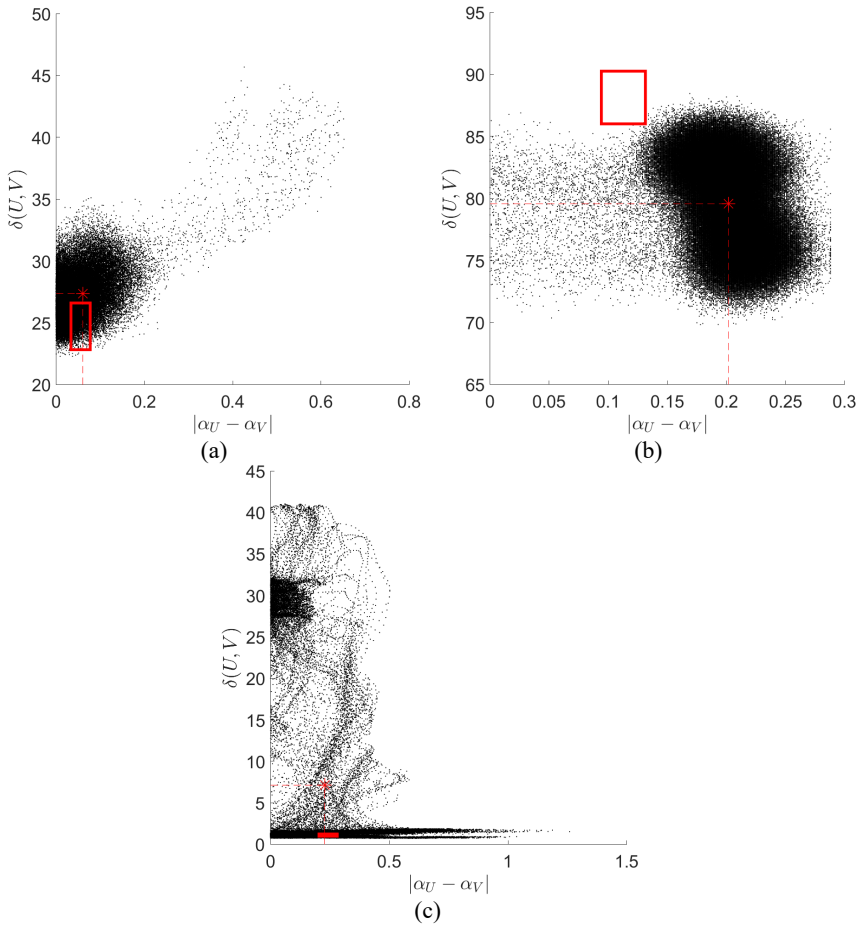
Fig. 4.2. Tested texture image is recognized as defective:
(a) ceramic tile; (b) fabric scrap; (c) glass sheet

Tables 4.1 and 4.3 present the classification results obtained for different texture surfaces, with variable size of image fragments U and V.

Summing up, the research shows that the best classification results for the class of ceramic tiles are obtained when the size of U is 16×16 and the size of fragment V is 32×32. Meanwhile, the best results for glass sheets and fabric scraps are obtained when the size of U is 32×32 and the size of V is 64×64. The texture defect detection accuracy is found to be: 0.95 (ceramic tiles), 0.67 (fabric scraps), 0.96 (glass sheets). It should be noted that the analysis of various size fragments (U and V) does not indicate any significant changes in the results.

Table 4.1. Ceramic tile classification results based on fragmentary smoothness and similarity

	16×16 (*U*), 32×32 (*V*)					32×32 (*U*), 64×64 (*V*)					64×64 (*U*), 128×128 (*V*)				
	1	2	3	4	5	1	2	3	4	5	1	2	3	4	5
TP	100	100	100	100	100	100	100	98	100	98	92	94	90	98	96
FP	8	12	10	10	12	10	14	12	10	8	10	10	10	10	8
TN	92	88	90	90	88	90	86	88	90	92	90	90	90	90	92
FN	0	0	0	0	0	0	0	2	0	2	8	6	10	2	4

Table 4.2. Fabric scrap classification results based on fragmentary smoothness and similarity

	16×16 (*U*), 32×32 (*V*)					32×32 (*U*), 64×64 (*V*)					64×64 (*U*), 128×128 (*V*)				
	1	2	3	4	5	1	2	3	4	5	1	2	3	4	5
TP	40	47	40	37	40	40	53	47	33	43	33	47	40	27	37
FP	13	7	7	13	3	13	7	7	13	3	3	10	10	7	7
TN	87	93	93	87	97	87	93	93	87	97	97	90	90	93	93
FN	60	53	60	63	60	60	47	53	67	57	67	53	60	73	63

Table 4.3. Glass sheet classification results based on fragmentary smoothness and similarity

	16×16 (*U*), 32×32 (*V*)					32×32 (*U*), 64×64 (*V*)					64×64 (*U*), 128×128 (*V*)				
	1	2	3	4	5	1	2	3	4	5	1	2	3	4	5
TP	92	94	86	84	90	94	96	96	96	96	82	86	78	84	80
FP	6	8	6	8	14	4	2	0	4	2	8	8	4	10	6
TN	94	92	94	92	86	96	98	100	96	98	92	92	96	90	94
FN	8	6	14	6	10	6	4	6	6	6	18	14	22	16	20

4.4. Chapter conclusions

The preliminary experimental results show that the established relationships between image smoothness and image similarity can be employed in the context of defect detection for texture images.

This proposed approach (method) is best suited for classifying ceramic tile and glass sheet products which can be characterised as very noisy and/or smooth enough.

It is important to mention that the theoretical and experimental analysis indicates minor fragment changes caused by minor changes in the image smoothness parameter (the necessary image similarity condition). Thus, in general, the image similarity clause can be also explored to reduce the scale of computing for the image testing process.

Of course, this method requires extensive additional studies and optimization procedures to be ready to implement it in a real defect detection system. First of all, this approach should be implemented using some lower level programming language.

In parallels, it can be observed that in this case the computational complexity of texture defect detection process is $O(6 \times 10^7 N^2)$, for image of size $N \times N$.

5. CONCLUSIONS

1. Most of the texture defect detection methods proposed and described in other literature sources focus on specific image texture classes. Considering the fact that the characteristics of textures belonging to the same class can differ significantly, it is expedient to apply a more flexible (parameterized) defect detection and localization technique.
2. The analysis of the overall performance of various discrete wavelet (Haar, LeGall, Daubechies D4) transform (DWT) application for testing texture images reveals that the discrete Haar wavelet transform provides better test results by on average 7–21 % in comparison with other DWT. This can be explained by the fact that Haar wavelets are "square" shaped, i.e. are not continuous. It is regarded as an advantage when analysing signals (images) which are characterised by sudden transitions (contrast changes). The latter condition is mainly common for the defective texture images.
3. Since the decision about the quality of the texture surface (image) in the proposed defect detection technique is based on a multiple image scanning by simultaneously applying a different two-dimensional discrete Haar wavelet filter, a relatively high (83–98 %) and competitive image testing accuracy is guaranteed.
4. A novel algorithm for computing discrete Haar spectra for the selected texture image fragments is proposed. The algorithm appears to be 10–20 times faster than direct estimation procedures. This is particularly important in real-time applications (defect localization in texture images, locally progressive image coding, etc.).
5. An important fact which allows improving the effectiveness of the whole texture defect detection and localization process (in terms of time input up to 20 %) is a possibility to use a priori generated subsets of multi-valued defect detection criterion for defect localization on surfaces which are characterised by fine or regular texture.
6. The performed experimental research revealed that the application of the newly developed statistically-based multi-valued texture defect detection criterion allows obtaining a relatively high mean accuracy of image (surface) quality evaluation, in particular (system parameter $p = 0.99$): 0.98 (class of glass sheets); 0.97 (class of ceramic tiles); 0.83 (class of textile products characterised by a strongly expressed directional texture). The obtained results are assumed to be good and competitive in comparison with the defect detection methods presented in other literature sources.

7. This dissertation also provides an alternative texture defect detection technique by employing the image fragment smoothness and similarity relations. Even though this approach is implementable, the obtained results of texture quality testing are considered to be worse (2–13 %) in comparison with the results recorded in the spectral Haar wavelet domain, i.e. by applying a multiple-valued defect detection criterion.

REFERENCES

1.   BU H. G., HUANG X. B., WANG J., CHEN X. Detection of fabric defects by auto-regressive spectral analysis and support vector data description. *Textile Research Journal*. 2010, 80(7), 579–589. ISSN 0040-5175.

2.   BU H. G., HUANG X. B. A novel multiple fractal features extraction framework and its application to the detection of fabric defects. *Journal of the Textile Institute*. 2008, 99(5), 489–497. ISSN 0040-5000.

3.   CHEN S. G., LIN B., HAN X. S., LIANG X. H. Automated inspection of engineering ceramic grinding surface damage based on image recognition. *International Journal of Advanced Manufacturing Technology*. 2013, 66(1–4), 431–443. ISSN 0268-3768.

4.   CHEN S. H., PERNG D. B. Directional textures auto-inspection using principal component analysis. *International Journal of Advanced Manufacturing Technology*. 2011, 55(9-12), 1099–1110. ISSN 0268-3768.

5.   CHUANG W. L., CHEN C. H., YEN J. Y., HSU Y. L. Using MPCA of spectra model for fault detection in a hot strip mill. *Journal of Materials Processing Technology*. 2009, 209(8), 4162–4168. ISSN 0924-0136

6.   ELBEHIERY H., HEFNAWY A., ELEWA M. Surface defects detection for ceramic tiles using image processing and morphological techniques. *Proceedings of World Academy of Science, Engineering and Technology*. 2005, 5, 158–162. ISSN 1307-6884.

7.   GUAN S. Q., GAO Z. Y. Fabric defect image segmentation based on the visual attention mechanism of the wavelet domain. *Textile Research Journal*. 2014, 84(10), 1018–1033. ISSN 0040-5175.

8.   HADIZADEH H., SHOKOUHI S. B. Random texture defect detection using 1-D hidden Markov models based on local binary patterns. *IEICE Transactions on Information and Systems*. 2008, E91D(7), 1937–1945. ISSN 0916-8532.

9.   HANMANDLU M., CHOUDHURY D., DASH S. Detection of defects in fabrics using topothesy fractal dimension features. *Signal Image and Video Processing*. 2015, 9(7), 1521–1530. ISSN 1863-1703.

10.   HOSEINI E., FARHADI F., TAJERIPOUR F. Fabric defect detection using

auto-correlation function. *International Journal of Computer Theory and Engineering*. 2013, 5(1), 114–117. ISSN 1793-8201.

11. HU C. S., MIN X., YUN H., WANG T., ZHANG S. K. Automatic detection of sound knots and loose knots on sugi using gray level co-occurrence matrix parameters. *Annals of Forest Science*. 2011, 68(6), 1077–1083. ISSN 1286-4560.

12. HU G. H. Automated defect detection in textured surfaces using optimal elliptical Gabor filters. *Optik – International Journal for Light and Electron Optics*. 2015, 126(14), 1331–1340. ISSN 0030-4026.

13. HU G. H., ZHANG G. H., Wang Q. H. Automated defect detection in textured materials using wavelet-domain hidden Markov models. *Optical Engineering*. 2014, 53(9), 093107-1-17. ISSN 0091-3286.

14. KARIMI M. H., ASEMANI D. Surface defect detection in tiling industries using digital image processing methods: Analysis and evaluation. *ISA Transactions*. 2014, 53(3), 834–844. ISSN 0019-0578.

15. KWON B. K., WON J. S., KANG D. J. Fast defect detection for various types of surfaces using random forest with VOV features. *International Journal of Precision Engineering and Manufacturing*. 2015, 16(5), 965–970. ISSN 2234-7593.

16. LIU X., SU Z. W. Z., CHOI K. F. Slub extraction in woven fabric images using Gabor filters. *Textile Research Journal*. 2008, 78(4), 320–325. ISSN 0040-5175.

17. MAK K. L., PENG P., YIU K. F. C. Fabric defect detection using morphological filters. *Image and Vision Computing*. 2009, 27(10), 1585–1592. ISSN 0262-8856.

18. MAK K. L., PENH P. An automated inspection system for textile fabrics based on Gabor filters. *Robotics and Computer-Integrated Manufacturing*. 2008, 24(3), 359–369. ISSN 0736-5845.

19. NAJAFABADI F. S., POURGHASSEM H. Corner defect detection based on dot product in ceramic tile images. *IEEE 7th International Colloquium on Signal Processing and its Applications, 2011 CSPA, March 4-6, Penang, Malaysian*. New York: IEEE, 2011, 293–297. ISBN 978-1-61284-414-5.

20. NGAN H. Y. T., PANG G. K. H., YUNG N. H. C. Automated fabric defect detection – A review. *Image and Vision Computing*. 2011, 29(7), 442–458. ISSN 0262-8856.

21. RAHEJA J. L., AJAY B., CHAUDHARY A. Real time fabric defect detection system on an embedded DSP platform. *Optik – International Journal for Light and Electron Optics*. 2013a, 124(21), 5280–5284. ISSN 0030-4026.

22. SAEIDI R. G., OUKIL A., AMIN G. R., RAISSI S. Prioritization of textile fabric defects using ordered weighted averaging operator. *International*

Journal of Advanced Manufacturing Technology. 2015, 76(5-8), 745–752. ISSN 0268-3768.

23. SHAM F. C., CHEN N., LONG L. Surface crack detection by flash thermography on concrete surface. *Insight*. 2008, 50(5), 240–243. ISSN 1354-2575.

24. SONG K., YAN Y. A noise robust method based on completed local binary patterns for hot-rolled steel strip surface defects. *Applied Surface Science*. 2013, 285P, 858–864. ISSN 0169-4332.

25. TAJERIPOUR F., FEKRI-ERSHAD S. Developing a novel approach for stone porosity computing using modified local binary patterns and single scale retinex. *Arabian Journal for Science and Engineering*. 2014, 39(2), 875–889. ISSN 1319-8025.

26. TIMMA F., BARTHA E. Non-parametric texture defect detection using Weibull features. *Image Processing: Machine Vision Applications IV, Vol. 7877. Proceedings of SPIE*. San Francisco: SPIE-IS&T, 2011. ISBN 978-0-8194-8414-7.

27. TOLBA A. S. A novel multiscale-multidirectional autocorrelation approach for defect detection in homogeneous flat surfaces. *Machine Vision and Applications*. 2012, 23(4), 739–750. ISSN 0932-8092.

28. TSAI D. M., CHEN M. C., LI W. C., CHIU W. Y. A fast regularity measure for surface defect detection. *Machine Vision and Applications*. 2012, 23(5), 869–886. ISSN 0932-8092.

29. TSAI D. M., LAI S. C. Defect detection in periodically patterned surfaces using independent component analysis. *Pattern Recognition*. 2008, 41(9), 2812–2832. ISSN 0031-3203.

30. VAIDELIENĖ G., VALANTINAS J. On the detection of self-similarities in vibro-acoustic signals. Journal of Vibroengineering. 2015, 17(8), 4259–4268. ISSN 1392-8716.

31. VALANTINAS J., KANČELKIS D., VALANTINAS R., VIŠČIŪTĖ G. Improving space localization properties of the discrete wavelet transform. *Informatica*. 2013, 24(4), 657–674. ISSN 0868-4952.

32. XIE X. A review of recent advances in surface defect detection using texture analysis techniques. *Electronic Letters on Computer Vision and Image Analysis*. 2008, 7(3), 1–22. ISSN 1577-5097.

33. XIE X., MIRMEHDI M., THOMAS B. Colour tonality inspection using eigenspace features. *Machine Vision and Applications*. 2006, 16(6), 364–373. ISSN 0932-8092.

34. YUAN X. C., WU L. S., PENG Q. J. An improved Otsu method using the weighted object variance for defect detection. *Applied Surface Science*. 2015, 349, 472–484. ISSN 0169-4332.

35. ŽUMBAKIS T., VALANTINAS J. Definition, evaluation and task-oriented application of image smoothness estimates. *Information Technology and Control*. 2004, 31(2), 16–23. ISSN 1392-124X.

LIST OF AUTHOR'S PUBLICATIONS

Papers in Master List Journals of the Institute of Scientific Information (ISI)

1. VALANTINAS J., KANČELKIS D., VALANTINAS R., VIŠČIŪTĖ G. Improving space localization properties of the discrete wavelet transform // *Informatica*. Vilnius: Institute of Mathematics and Informatics. ISSN 0868-4952. 2013, Vol. 24, no. 4, p. 657-675. [Science Citation Index Expanded (Web of Science); INSPEC; MatSciNet; Scopus; Zentralblatt MATH] [M.kr. 01P]. [Indėlis: 0,250]. [IF (E): 0,901 (2013)]
2. VAIDELIENĖ G., VALANTINAS J. On the detection of self-similarities in vibro-acoustic signals // *Journal of vibroengineering*. Kaunas: JVE International. ISSN 1392-8716. 2015, vol. 17, iss. 8, p. 4259-4267. [Science Citation Index Expanded (Web of Science); Inspec; Academic Search Complete; Central & Eastern European Academic Source (CEEAS); Computers & Applied Sciences Complete; Current Abstracts; TOC Premier] [M.kr. 01P]. [Indėlis: 0,500]. [IF (E): 0,384 (2015)]
3. VAIDELIENĖ G., VALANTINAS J., RAŽANSKAS P. On the use of discrete wavelets in implementing defect detection system for texture images // *Informacinės technologijos ir valdymas = Information technology and control*. Kaunas: KTU. ISSN 1392-124X. 2016, t. 45, Nr. 2, p. 214-222. [Science Citation Index Expanded (Web of Science); INSPEC; Scopus] [M.kr. 01P]. [Indėlis: 0,333]. [IF (E): 0,633 (2015)]
4. VAIDELIENĖ G., VALANTINAS J. The use of Haar wavelets in detecting and localizing texture defects // *Image analysis & stereology*. Ljubljana: International Society for Stereology. ISSN 1580-3139. 2016, vol. 35, iss. 3, p. 195-201. [Science Citation Index Expanded (Web of Science); Current Contents (Engineering, Computing & Technology)]. [Indėlis: 0,500]. [IF (E): 0,500 (2015)]

Publications in peer-reviewed journals and conferences

1. VAIDELIENĖ G., VALANTINAS J. Haar wavelet-based approach to locating defects in texture images // *Information and software technologies: proceedings of the 21st international conference*, ICIST 2015, Druskininkai,

Lithuania, October 15-16, 2015. Cham: Springer, 2015. (Communications in computer and information science, Vol. 538, ISSN 1865-0929), ISBN 9783319247694. p. 537-547. [0,500]

2. VAIDELIENĖ G., VALANTINAS J. Wavelet-based defect detection system for grey-level texture images // VISIGRAPP 2016: proceedings of the 11th joint conference on computer vision, imaging and computer graphics theory and applications, Vol. 4: VISAPP, Rome, Italy, February 27-29, 2016. Setúbal: SCITEPRESS - Science and technology publications, ISBN 9789897581755. p. 143-149. [0,500]

INFORMATION ABOUT THE AUTHOR

Date of birth: 29 November 1987, Kaunas.
Education:
2006–2010 m. – Bachelor in Science of Applied mathematics, Faculty of Fundamental Science, Kaunas University of Technology.
2010–2012 m. – Master in Science of Applied mathematics, Faculty of Fundamental Science, Kaunas University of Technology.
2012–2016 m. – Doctoral studies in Physical Sciences (Informatics 09P), Department of Applied Mathematics, Faculty of Mathematics and Natural Sciences.
Teaching experience:
Since 2013 Assistant, Department of Applied Mathematics, Faculty of Mathematics and Natural Sciences, Kaunas University of Technology.
Research interests:
Image analysis, wavelet theory, fractal technologies and time series forecasting techniques.
E-mail
gintare.vaideliene@ktu.lt

REZIUMĖ

Skaitmeninių vaizdų analizei skiriamas dėmesys per pastaruosius dešimtmečius gerokai išaugo. Vaizdai, kaip geriausiai žmogui suvokiama informacijos forma, giliai prasiskverbė į tokias veiklos sritis kaip medicina, mikroskopija, astronomija, robotika, gynybos pramonė ir kt.

Žmogiškojo vaizdų suvokimo proceso interpretacija, analizė ir apdorojimas bei analogiško veikimo mechanizmo realizavimas kompiuteriu sparčiai auga. Ištobulėjus kompiuterinei technikai, atsirado galimybė realizuoti bei praktiškai taikyti sudėtingus vaizdų apdorojimo metodus ir technologijas. Labai svarbu pakeisti žmogaus veiklą tose srityse, kurios reikalauja ilgo, įtempto sudėtingomis sąlygomis žmogaus darbo. Viena tokių sričių yra kokybės kontrolės

optimizavimas pramoniniame procese, dažnai besiremiantis vizualiąja skaitmeninių vaizdų analize.

Kokybės kontrolė – labai svarbus aspektas šiandieninėje konkurencingoje pramonėje. Kokybės sąvoką apibrėžia tarptautinis standartas ISO 9000 – tai „visuma produkcijos savybių ir charakteristikų arba paslaugų, kurios užtikrina galimybę patenkinti nustatytus arba numanomus poreikius".

Vienas iš būdų siekiant pagerinti galutinio produkto kokybę yra užtikrinti kiekvieno gamybos proceso etapo efektyvumą. Įvairių pramonės gaminių paviršiaus (tekstūrinių vaizdų) defektai daugiausia aptinkami žmonėms – inspektoriams padedant. Deja, toks būdas yra labai subjektyvus, lėtina visą gamybos procesą, todėl jis tampa brangus ir atimantis daug laiko. Nustatyta, jog žmogaus efektyvumas, nustatant gaminio kokybę, siekia 60–75 %. Todėl aktualu šį procesą automatizuoti bei kurti efektyvius metodus tekstūrinių paviršių (vaizdų) defektams nustatyti.

Defektų aptikimo metodika tekstūriniuose vaizduose, tokiuose kaip popierius, stiklo lakštai, keraminės plytelės, audiniai, oda, plastiko produkcija, yra glaudžiai susijusi su skaitmeninių vaizdų apdorojimo procedūromis. Literatūroje siūloma įvairių požiūrių ir technologijų šiai problemai spręsti. Visus juos galima suskirstyti į kelias grupes, būtent: statistinis, spektrinė tekstūros analizė, modeliais grindžiamas ir struktūrinis požiūriai. Taip pat galima išskirti metodus, kurie skirti aptikti specifinius tekstūros defektus: skyles, dėmes, įtrūkimus, spalvos toną ir pan. Nors šiuo metu didėja poreikis kurti sistemas, kurios geba analizuoti bei identifikuoti įvairias tekstūras ir jų plataus spektro defektus.

Darbe pasiūlyta nauja, originali tekstūrinių vaizdų (paviršių) defektų aptikimo metodika, kuri realizuota spektrinėje diskrečiųjų bangelių srityje. Beje, diskrečiosios bangelės šiuo metu yra vienas populiariausių ir efektyviausių analizės metodų. Pasiūlyta tekstūros defektų aptikimo metodika sėkmingai pritaikyta realių tekstūrinių paviršių tyrimams bei jų kokybės kontrolei.

Darbo objektas – diskrečiųjų bangelių teorija grindžiami tekstūrinių paviršių (vaizdų) klasifikavimo metodai.

Darbo tikslas – sukurti lanksčią tekstūrinių vaizdų kokybės įvertinimo spektrinėje diskrečiųjų bangelių srityje metodiką bei adaptuoti ją realioms gaminių kokybės testavimo sistemoms.

Darbo uždaviniai

Darbo tikslui pasiekti iškelti tokie uždaviniai:

(1) suformuoti tekstūros defektų aptikimo spektrinėje diskrečiųjų bangelių srityje kriterijus bei pateikti metodiką;

(2) išanalizuoti įvairių diskrečiųjų bangelių transformacijų (DBT) panaudojimo tekstūrinių vaizdų kokybei tirti galimybes;

(3) sudaryti DBT spektro greito apskaičiavimo pasirinktiems tekstūrinio

vaizdo fragmentams procedūrą;

(4) pasiūlyti efektyvią tekstūros defektų lokalizavimo metodiką;

(5) sukurti parametrizuotą sistemą, leidžiančią testuoti tekstūrinius vaizdus ir lokalizuoti juose aptiktus defektus;

(6) ištirti sukurtos sistemos efektyvumą atskiroms tekstūrinių vaizdų klasėms (šaligatvio plytelės, stiklo gaminiai, tekstilės audiniai ir kt.);

(7) atliktų tyrimų kontekste aptarti kitus galimus tekstūros defektų aptikimo problemos sprendimo būdus.

Tyrimų metodai ir programinė įranga

Darbe taikomi matriciniai skaičiavimai, diskrečiųjų bangelių analizės metodai bei matematinės statistikos priemonės (parametrų įverčiai, statistinės hipotezės).

Eksperimentai realizuoti *Matlab R2014a* aplinkoje.

Darbo mokslinis naujumas

Disertacijoje pasiūlyta keletas naujų sprendimų, užtikrinančių efektyvią tekstūros defektų aptikimo spektrinėje diskrečiųjų bangelių srityje sistemos realizaciją. Jie tokie.

(1) Pasiūlyta tekstūros defektų aptikimo metodika remiasi daugkartiniu apdorojamo tekstūrinio vaizdo skenavimu, o visi žinomi (literatūroje sutinkami) metodai apsiriboja vienkartine vaizdo (ar jo diskrečiojo bangelių spektro, jei taikoma bangelių transformacija) analize. Daugkartinis vaizdo skenavimas leidžia suformuoti daugiareikšmį tekstūrinių vaizdų defektų aptikimo kriterijų, kai sprendimas apie apdorojamo tekstūrinio vaizdo kokybę siejamas su procentiniu palankių ir nepalankių teigiamai išvadai apie vaizdo kokybę priimti kriterijaus reikšmių santykiu.

(2) Panaudota statistinė tikslingai orientuota tekstūrinio vaizdo diskrečiosios Haar transformacijos koeficientų poaibių analizė leido realizuoti tekstūros defektų aptikimo sistemą (metodiką), kuri geba valdyti kokybiškų ir nekokybiškų vaizdų klasifikavimo procesą, tokiu būdu užtikrinant sistemos lankstumą.

(3) Tekstūros defektams lokalizuoti taikomi tie patys defektų aptikimo tekstūriniuose vaizduose kriterijai bei analizės principai, t. y. panaudojami jau suformuoto daugiareikšmio tekstūros defektų aptikimo kriterijaus poaibiai.

(4) Pasiūlytas naujas atskirų tekstūrinio vaizdo fragmentų diskrečiojo Haar spektro apskaičiavimo algoritmas. Algoritmo efektyvumą ir greitį sąlygoja tai, jog didžioji dalis spektrinių Haar koeficientų tiesiog atrenkami iš viso vaizdo Haar spektro. Tai ypač svarbu tais atvejais, kai tekstūros defekto lokalizavimas vyksta realiuoju laiku.

Ginamieji teiginiai

(1) Sprendimas dėl tekstūrinio vaizdo kokybės priimamas remiantis daugkartinio vaizdo skenavimo rezultatais, kai kiekvienąkart panaudojami skirtingi dvimačiai diskrečiųjų bangelių filtrai. Tai užtikrina gana aukštą (83–98 %) testavimo tikslumą.

(2) Pasiūlytas originalus diskrečiojo Haar spektro apskaičiavimo pasirinktiems tekstūrinio vaizdo fragmentams algoritmas, įvertinus greičio išlošį, yra 10–30 kartų efektyvesnis už tiesiogines fragmentinio spektro radimo procedūras.

(3) Aptikti tekstūros defektai lokalizuojami, panaudojant tikslingai atrinktus jau suformuoto daugiareikšmio defektų aptikimo kriterijaus poaibius.

(4) Eksperimento rezultatai, gauti taikant naujai sukurtą tekstūros defektų aptikimo ir lokalizavimo sistemą, patvirtino pasiūlytų sprendimų patrauklumą ir efektyvumą.

Darbo rezultatų praktinė reikšmė

Disertacijoje pateikti sprendimai – vaizdų tekstūros analizė, panaudojant dvimačius diskrečiųjų bangelių filtrus, originalus pasirinktų vaizdo fragmentų Haar spektro apskaičiavimo algoritmas, tekstūros defektų aptikimo kriterijaus formavimo principai gali būti sėkmingai panaudoti ne tiktai tekstūros defektų aptikimo ir lokalizavimo procesams, bet ir kitose su skaitmeninių vaizdų apdorojimu susijusiose srityse, tokiose kaip objektų lokalizavimas gardelinę struktūrą turinčiuose vaizduose, lokaliai progresyvus vaizdų kodavimas, vaizdo požymių išskyrimas ir pan.

Būtina pabrėžti, jog pasiūlyta tekstūros defektų aptikimo ir lokalizavimo metodika leidžia klasifikuoti tekstūrinius vaizdus bei lokalizuoti juose aptiktus defektus realiuoju laiku. Tai ypač svarbu, kai kalbama apie automatizuotas pramonines tekstūrinių paviršių testavimo sistemas.

Disertacijos rezultatų aprobavimas

Disertacijos tema paskelbti 6 moksliniai straipsniai, iš jų 4 tarptautiniuose žurnaluose su citavimo indeksais, referuojamuose Mokslinės informacijos instituto (ISI) pagrindiniame sąraše, kiti – konferencijų medžiagoje. Tyrimai disertacijos tema pristatyti 2 tarptautinėse ir 2 nacionalinėse konferencijose.

Disertacijos struktūra

Daktaro disertaciją sudaro įvadas, 4 pagrindiniai skyriai, išvados, literatūros sąrašas ir mokslinių publikacijų sąrašas. Disertacijos teksto apimtis – 104 puslapiai. Disertacijos pagrindinėje dalyje yra 35 iliustracijos, 13 lentelių. Rengiant disertaciją pasitelkti 145 literatūros šaltiniai.